RESEARCH ARTICLE
SPACE PHYSICS

Earth and Planetary Physics
10: 269–279, 2026
doi: 10.26464/epp2026028

Transformations of space electromagnetic fields in different non-inertial reference frames and their applications

Chao Shen[1*], and Yong Ji[2]

[1]College of Science, Harbin Institute of Technology (Shenzhen), Shenzhen 518055, China;

[2]School of Mathematics and Statistics, Ningxia University, Yinchuan 750021, China

Key Points:

- Universal formulas are derived for electromagnetic field transformations.
- Galilean transformations are found valid for low-speed space plasmas.
- The Poisson equation is shown applicable to calculations of MMS charge density.

Citation: Shen, C., and Ji, Y. (2026). Transformations of space electromagnetic fields in different non-inertial reference frames and their applications. *Earth Planet. Phys.*, *10*(2), 269–279. http://doi.org/10.26464/epp2026028

Abstract: How to transform an electromagnetic field across non-inertial frames of reference is a common challenge encountered in electromagnetic space measurements and analyses. Finding clear and precise ways to evaluate transformation formulas can be difficult. This study presents results of a thorough theoretical investigation that has yielded universal transformation formulas; these transformations are successfully applied to two specific scenarios. We find that, for space plasmas, if the relative velocities of structures are significantly lower than the speed of light, Galilean transformations are suitable. The transformations presented in this paper are applicable, in low speed situations, to electromagnetic fields, electric potentials and magnetic vector potentials, and to charge density and current density, measured in various non-inertial reference frames. Truncation errors associated with these simplified transformations are calculated and shown to be acceptable. These findings have broad implications for space physics measurements and analyses. We address two key issues related to non-inertial frame transformations: first, how to derive a general formula for the rotational electric potential of planets with intrinsic magnetic fields; second, how to verify rigorously the calculation of charge density from MMS (Magnetospheric Multiscale) electrostatic field measurements. We suggest that, due to the validity of the Coulomb gauge, the Poisson equation can be applied in situations of low-speed motion, allowing MMS measurement data to be used to calculate minimal-error charge density.

Keywords: transformation of electromagnetic fields; space physics; charge density in space

1. Introduction

To study physical processes in space, it is essential to choose a specific frame of reference suitable to the question being addressed. Space–time reference systems are divided into inertial and non-inertial categories. An inertial reference system is one that remains stationary or moves uniformly in space and time. For example, the heliocentric (centered around the sun) reference frame, used to measure and study the orbital motion of planets within the solar system, is an inertial frame that is also suitable for describing the motion of solar wind. Likewise, the geocentric (celestial Earth-centered) reference system is often used as an inertial frame when studying the impact of solar wind on Earth's magnetosphere. A satellite or space station in free orbit around Earth can also serve as a local inertial frame due to its condition of weightlessness, as explained by the equivalence principle (Misner et al., 1973). In these frames, matter's motion follows the laws of physics in flat spacetime, and observed electromagnetic fields comply with Lorentz transformations (Misner et al., 1973). Conversely, frames experiencing non-uniform motion are non-inertial. For analysing solar wind turbulence, a reference system moving with the low-pass filtering solar wind velocity is used; this reference frame is non-inertial due to variations of the solar wind speed. To study spatial characteristics of the Earth's geomagnetic field, the Earth-body reference system is employed, in which the Earth's magnetic field appears stationary; but this system is rotational and non-inertial due to Earth's rotation. Some space exploration satellites, because they are spinning, also operate in non-inertial reference systems. In a non-inertial frame, an equivalent gravitational field exists, making spacetime curved and causing physical phenomena to follow the laws suitable to curved space–time (Misner et al., 1973).

Non-inertial frames are prevalent in space electromagnetic measurements, analyses, and applications. Transforming electromagnetic fields between non-inertial reference frames is crucial in space exploration and theoretical analysis. This paper presents a

Correspondence to: C. Shen, shenchao@hit.edu.cn
Received 16 OCT 2025; Accepted 07 JAN 2026.
First Published online 06 FEB 2026.

systematic and comprehensive analysis to establish the general transformation relationship among electromagnetic field quantities in different non-inertial reference frames. In Sections 2 and 3, we develop electromagnetic field transformations in a hierarchical manner, starting from the exact Lorentz transformation, proceeding to its low-speed approximation, and finally reducing the approximation to the Galilean transformation appropriate for study of macroscopic space plasma motions. Sections 4 and 5 present two applications: determining the rotational electric potential of planets, and measuring space net charge density. Our conclusions are summarized in Section 6.

2. General Transformations Among Electromagnetic Field Quantities in a Low-speed Moving Reference System

Measurement of electromagnetic field quantities varies with choice of reference system; how to transform measurements between different systems is clear. It is important to note that the velocities and accelerations associated with non-inertial reference frames in space physics are generally quite small compared to the speed of light. In a non-inertial frame, if the equivalent gravitational potential is denoted as φ and the relative velocity of frames is denoted as u, the spacetime metric (line element) is expressed as

$$ds^2 = -(1+2\varphi/c^2)c^2dt^2 + (1+2\varphi/c^2)^{-1}(dx^2+dy^2+dz^2),$$

where t represents the time coordinate, (x, y, z) are the Cartesian spatial coordinates, and c is the speed of light in a vacuum (Padmanabhan, 2010). The impact of the equivalent gravitational effect on the non-inertial reference system is about

$$2\varphi/c^2 \sim u^2/c^2 \ll 1,$$

which is negligible for the macroscopic movements observed in space physics. For example, the Earth's co-rotating reference system deviates from flat spacetime by approximately

$$2\varphi/c^2 = \Omega^2 r^2/c^2 \sim 10^{-13},$$

where Ω is Earth's rotational angular velocity and r is the distance from the reference point to Earth's center.

Hence, non-inertial reference systems in space physics can generally be treated as Minkowski flat spacetimes, where the spacetime interval is

$$ds^2 = -c^2dt^2 + dx^2 + dy^2 + dz^2$$

and the metric tensor is diagonal {−1,1,1,1}. In this context, the physical laws applicable to Minkowski flat spacetime in inertial frames remain valid at high accuracy in non-inertial frames. This approach is also relevant in handling data collected by spin-stabilized satellites, where electromagnetic theory and Maxwell's equations for flat spacetime are accurate in the satellites' co-rotating observational frames. The transformation of physical quantities between different reference systems (whether inertial or non-inertial) thus closely follows the Lorentz transformation (Misner et al., 1973), with a negligible error margin $2\varphi/c^2 \sim u^2/c^2$.

Consider two reference frames, S and S', with spacetime coordinates in $(x^\mu) = \left(x^0 = ct, \boldsymbol{x}\right)$ and $(x'^\mu) = \left(x'^0 = ct', \boldsymbol{x}'\right)$, respectively. Here $\mu = (0, 1, 2, 3)$ denotes coordinate (t, x, y, z). The velocity of S' relative to S is $\boldsymbol{u}$, which varies with time and location. However, it is crucial to recognize that the Lorentz transformation, which applies between inertial frames, is valid only locally in spacetime and is not suitable for global transformations between non-inertial frames. The Lorentz transformation can be summarized as follows:

$$dx'^\mu = \frac{\partial x'^\mu}{\partial x^\nu}dx^\nu = \Lambda^\mu_\nu dx^\nu, \tag{1}$$

where the Lorentz transformation matrix is

$$\Lambda^\mu_\nu = \frac{\partial x'^\mu}{\partial x^\nu} = \begin{pmatrix} \gamma & -\gamma\beta_j \\ -\gamma\beta_i & \delta_{ij} + \dfrac{\gamma^2}{\gamma+1}\beta_i\beta_j \end{pmatrix}, \tag{2}$$

where $\beta_i = u_i/c$ (vector form $\boldsymbol{\beta} = \boldsymbol{u}/c$), the Lorentz factor is $\gamma = \left(1-\beta^2\right)^{-\frac{1}{2}}$.

The matrix of the inverse Lorentz transformation is

$$\hat{\Lambda}^\mu_\nu = \frac{\partial x^\mu}{\partial x'^\nu} = \begin{pmatrix} \gamma & \gamma\beta_j \\ \gamma\beta_i & \delta_{ij} + \dfrac{\gamma^2}{\gamma+1}\beta_i\beta_j \end{pmatrix}, \tag{3}$$

where $i, j = (1, 2, 3)$ denotes space coordinate (x, y, z), and δ_{ij} is the Kronecker delta which equate 1 for $i = j$ and 0 for $i \neq j$.

All these transformations adhere to the principles of special relativity (D'Auria and Trigiante, 2011). Physical scalars such as charge (Q), particle number, distribution function, and phase shift are relativistic invariants, meaning they are preserved under arbitrary transformation. However, four-dimensional (4D) vectors p^μ such as 4-velocity $(\gamma c, \gamma\boldsymbol{v})$, 4-vector potential $(\phi/c, \boldsymbol{A})$, 4-current density $(c\rho, \boldsymbol{j})$, and 4-wave vector $(\nu/c, \boldsymbol{k})$ are frame-dependent and undergo Lorentz transformation from one frame to another (S to S') as follows:

$$p'^\mu = \Lambda^\mu_\nu p^\nu. \tag{4}$$

The transformation of the electromagnetic tensor $F^{\mu\nu}$ ($F_{\alpha\beta} \equiv \partial_\alpha A_\beta - \partial_\beta A_\alpha$) is

$$F'^{\mu\nu} = \Lambda^\mu_\lambda \Lambda^\nu_\sigma F^{\lambda\sigma}. \tag{5}$$

Specifically, the local transformation of the spacetime coordinate is

$$d\boldsymbol{x}' = d\boldsymbol{x} + \frac{\gamma^2}{(\gamma+1)c^2}(\boldsymbol{u}\cdot d\boldsymbol{x})\boldsymbol{u} - \gamma\boldsymbol{u}dt, \tag{6}$$

$$dt' = \gamma\left(dt - \boldsymbol{u}\cdot d\boldsymbol{x}/c^2\right). \tag{7}$$

Dividing (6) by (7), the superposition law of velocities is obtained as follows:

$$\boldsymbol{v}' = \frac{1}{1-\boldsymbol{v}\cdot\boldsymbol{u}/c^2}\left[\frac{1}{\gamma}\boldsymbol{v} - \boldsymbol{u} + \frac{\gamma}{\gamma+1}\cdot\frac{(\boldsymbol{v}\cdot\boldsymbol{u})\boldsymbol{u}}{c^2}\right]. \tag{8}$$

The transformation of electric current density and charge density between different reference frames is expressed as

$$\begin{cases}\rho' = \gamma\left(\rho - \boldsymbol{u}\cdot\boldsymbol{j}/c^2\right),\\ \boldsymbol{j}' = \boldsymbol{j} - \gamma\rho\boldsymbol{u} + \dfrac{\gamma^2}{(\gamma+1)c^2}(\boldsymbol{u}\cdot\boldsymbol{j})\,\boldsymbol{u}.\end{cases} \tag{9}$$

The transformation of electric potential and magnetic vector potential is

$$\begin{cases}\phi' = \gamma(\phi - \boldsymbol{u}\cdot\boldsymbol{A}),\\ \boldsymbol{A}' = \boldsymbol{A} - \dfrac{\gamma^2}{c^2}\phi\boldsymbol{u} + \dfrac{\gamma^2}{(\gamma+1)c^2}(\boldsymbol{u}\cdot\boldsymbol{A})\,\boldsymbol{u}.\end{cases} \tag{10}$$

The transformation of the electric field and the magnetic induction is

$$\begin{cases}\boldsymbol{E}' = \gamma\left(\boldsymbol{E} + \boldsymbol{u}\times\boldsymbol{B} - \dfrac{\gamma}{\gamma+1}(\boldsymbol{u}\cdot\boldsymbol{E})\,\boldsymbol{u}/c^2\right),\\ \boldsymbol{B}' = \gamma\left(\boldsymbol{B} - \dfrac{1}{c^2}\boldsymbol{u}\times\boldsymbol{E} - \dfrac{\gamma}{\gamma+1}(\boldsymbol{u}\cdot\boldsymbol{B})\,\boldsymbol{u}/c^2\right).\end{cases} \tag{11}$$

The transformation of electric displacement and magnetic field is

$$\begin{cases}\boldsymbol{D}' = \gamma\left(\boldsymbol{D} + \boldsymbol{u}\times\boldsymbol{H}/c^2 - \dfrac{\gamma}{\gamma+1}(\boldsymbol{u}\cdot\boldsymbol{D})\,\boldsymbol{u}/c^2\right),\\ \boldsymbol{H}' = \gamma\left(\boldsymbol{H} - \boldsymbol{u}\times\boldsymbol{D} - \dfrac{\gamma}{\gamma+1}(\boldsymbol{u}\cdot\boldsymbol{H})\,\boldsymbol{u}/c^2\right).\end{cases} \tag{12}$$

While the transformation of electric polarization intensity and magnetic polarization intensity between is

$$\begin{cases}\boldsymbol{P}' = \gamma\left(\boldsymbol{P} - \dfrac{1}{c^2}\boldsymbol{u}\times\boldsymbol{M} - \dfrac{\gamma}{\gamma+1}(\boldsymbol{u}\cdot\boldsymbol{P})\,\boldsymbol{u}/c^2\right),\\ \boldsymbol{M}' = \gamma\left(\boldsymbol{M} + \boldsymbol{u}\times\boldsymbol{P} - \dfrac{\gamma}{\gamma+1}(\boldsymbol{u}\cdot\boldsymbol{M})\,\boldsymbol{u}/c^2\right).\end{cases} \tag{13}$$

Doppler effect exists in the frequency and wave vector of fluctuations in different reference frames, and its transformation is

$$\begin{cases}\nu' = \gamma(\nu - \boldsymbol{u}\cdot\boldsymbol{k}),\\ \boldsymbol{k}' = \boldsymbol{k} - \dfrac{\gamma}{c}k\boldsymbol{u} + \dfrac{\gamma^2}{(\gamma+1)c^2}(\boldsymbol{u}\cdot\boldsymbol{k})\,\boldsymbol{u}.\end{cases} \tag{14}$$

To consider the transformation in the reverse direction (S' to S), we simply invert the velocity $\boldsymbol{u}$ in the formulas provided. For non-inertial reference frames, the transformation formula is valid for situations $u^2/c^2 \ll 1$, i.e., where the relative speed between frames is significantly less than the speed of light; Truncation errors are of the second order of u/c.

To ensure that the second-order error of u/c of the transformation formula is indeed minimized, a first-order u/c approximation is employed, neglecting terms of second order and higher. This simplifies the Lorentz transformation formulas. Consequently, the Lorentz transformation matrix and its inverse can be approximated as follows:

$$(\Lambda^{\mu}_{\nu}) = \begin{pmatrix}1 & -\beta_j\\ -\beta_i & \delta_{ij}\end{pmatrix}, \tag{15}$$

$$(\hat{\Lambda}^{\mu}_{\nu}) = \begin{pmatrix}1 & \beta_j\\ \beta_i & \delta_{ij}\end{pmatrix}. \tag{16}$$

The transformation of space–time coordinates becomes

$$\begin{cases}d\boldsymbol{x}' = d\boldsymbol{x} - \boldsymbol{u}dt,\\ dt' = dt - \dfrac{1}{c^2}\boldsymbol{u}\cdot d\boldsymbol{x},\end{cases} \tag{17}$$

and

$$\begin{cases}d\boldsymbol{x} = d\boldsymbol{x}' + \boldsymbol{u}dt',\\ dt = dt' + \dfrac{1}{c^2}\boldsymbol{u}\cdot d\boldsymbol{x}'.\end{cases} \tag{18}$$

Note that $\boldsymbol{u}$ can be variable with time and location.

Then, the relationship of the electric field and the magnetic induction in different reference frames approximates to

$$\begin{cases}\boldsymbol{E}' = \boldsymbol{E} + \boldsymbol{u}\times\boldsymbol{B},\\ \boldsymbol{B}' = \boldsymbol{B} - \dfrac{1}{c^2}\boldsymbol{u}\times\boldsymbol{E}.\end{cases} \tag{19}$$

The transformation of electric displacement and magnetic field becomes

$$\begin{cases}\boldsymbol{D}' = \boldsymbol{D} + \boldsymbol{u}\times\boldsymbol{H}/c^2,\\ \boldsymbol{H}' = \boldsymbol{H} - \boldsymbol{u}\times\boldsymbol{D}.\end{cases} \tag{20}$$

The approximated relationship of electric polarization intensity and magnetic polarization intensity is

$$\begin{cases}\boldsymbol{P}' = \boldsymbol{P} - \dfrac{1}{c^2}\boldsymbol{u}\times\boldsymbol{M},\\ \boldsymbol{M}' = \boldsymbol{M} + \boldsymbol{u}\times\boldsymbol{P}.\end{cases} \tag{21}$$

The approximated relationship of electric potential and magnetic vector potential is

$$\begin{cases}\phi' = \phi - \boldsymbol{u}\cdot\boldsymbol{A},\\ \boldsymbol{A}' = \boldsymbol{A} - \dfrac{1}{c^2}\phi\boldsymbol{u}.\end{cases} \tag{22}$$

The approximated relationship of charge density and electric current density is

$$\begin{cases}\rho' = \rho - \boldsymbol{u}\cdot\boldsymbol{j}/c^2,\\ \boldsymbol{j}' = \boldsymbol{j} - \rho\boldsymbol{u}.\end{cases} \tag{23}$$

The approximated relationship of frequency and wave vector of an electromagnetic wave is

$$\begin{cases}\nu' = \nu - \boldsymbol{k}\cdot\boldsymbol{u},\\ \boldsymbol{k}' = \boldsymbol{k} - \dfrac{1}{c}k\boldsymbol{u}.\end{cases} \tag{24}$$

The approximated formula for velocity superposition is

$$\boldsymbol{v}' = \boldsymbol{v} - \boldsymbol{u} + \boldsymbol{v}\frac{(\boldsymbol{v}\cdot\boldsymbol{u})}{c^2}. \tag{25}$$

The speed of light remains constant according to Equation (25) at this first-order approximation.

In typical space physics applications, the relative velocity between reference frames associated with macroscopic plasma structures, space craft motion, or planetary rotation rarely exceeds several tens to hundreds of kilometers per second. For example, taking a characteristic velocity $u\sim 50-500$ km/s, the corresponding dimensionless parameter is $u/c\sim 1.7\times10^{-4}-1.7\times10^{-3}$. Under these conditions, first order corrections proportional to u/c introduce relative errors of at most 10^{-3}, while second corrections propor-

tional to $(u/c)^2$ are typically smaller than 10^{-6}. For electromagnetic field transformations, this implies that the Galilean approximation introduces negligible errors for most macroscopic space plasma processes when compared with instrumental uncertainties. For instance, an electric field of magnitude $E\sim1$ mV/m would incur a transformation error on the order of 10^{-3} mV/m, which is well below the noise level of current spaceborne electric field instruments such as MMS/EDP.

Similarly, for charge density estimations derived from Gauss's law, a first order u/c error corresponds to a relative uncertainty typically smaller than 10^{-3}. Given that observed charge densities in space plasmas are already extremely small due to quasi-neutrality, this transformation-induced error remains below the detection threshold for most spacecraft constellations, except in regions with strong gradients or high vorticity. For wave phenomena, the Doppler frequency shift introduced by Galilean transformation scales as $\Delta\omega\sim\boldsymbol{k}\cdot\boldsymbol{u}$, while relativistic corrections scale as $(u/c)^2\omega$. For low frequency plasma waves and macroscopic structures, the latter term is negligible, confirming the validity of the classical Doppler approximation in most space plasma measurements.

These numerical estimates demonstrate that the first order u/c approximation provides a favorable balance between theoretical rigor and practical applicability; second order relativistic corrections are generally insignificant for low-speed space plasma processes. Consequently, the use of low speed Lorentz or Galilean transformations in the present study is well justified for the targeted applications.

3. Transformation for Space Electromagnetic Fields

Macroscopic motion in space is generally non-relativistic; also, the relative velocity between different frames is much lower than the speed of light. In common practical applications in space, the Galilean spacetime transformation simplifies the relationships of physical quantities between different frames and provides sufficient accuracy for measurement analysis and calculations.

3.1 Galilean Transformation for Spacetime

In non-relativistic situations, the relative speeds of motion between observed reference frames are generally much less than the speed of light, i.e., $u\ll c$, or $\beta_i=u_i/c\ll1$. Under this condition, the second order term in the time transformation formula within transformation Equations (17) and (18) is typically very small and can be neglected. This allows for the assumption that length and time remain effectively invariant across different reference frames. Consequently, the transformation of space–time coordinates adheres to the local Galilean transformation as follows:

$$\begin{cases} d\boldsymbol{x}' = d\boldsymbol{x} - \boldsymbol{u}dt, \\ dt' = dt, \end{cases} \tag{26}$$

and

$$\begin{cases} d\boldsymbol{x} = d\boldsymbol{x}' + \boldsymbol{u}dt', \\ dt = dt', \end{cases} \tag{27}$$

while the spacetime transform matrix and the corresponding inverse matrix become

$$(\Lambda^{\mu}_{\nu}) = \begin{pmatrix} 1 & 0 \\ -\beta_i & \delta_{ij} \end{pmatrix}, \tag{28}$$

$$(\Lambda^{-1\mu}_{\nu}) = \begin{pmatrix} 1 & 0 \\ \beta_i & \delta_{ij} \end{pmatrix}. \tag{29}$$

The determinant of the space–time coordinate transformation matrix and its inverse is approximately equal to 1, with errors up to the first order of u/c.

In scenarios involving such low-speed macroscopic motions common in space physics, the space–time coordinate complies with the local Galilean transformations, as illustrated in Equations (26) and (27). These approximate, Galilean, transformations are thus frequently used to examine macroscopic motion in space physics. According to Equation (26), the formula for velocity superposition is provided,

$$\boldsymbol{v}' = \boldsymbol{v} - \boldsymbol{u}. \tag{30}$$

In scenarios of low-speed motion, the measurement values from a clock and the length measured by a ruler remain constant across different frames of reference, aligning with Newton's concept of absolute space–time.

3.2 Galilean Transformations for Spacetime Gradients

The transformations of spacetime gradients satisfy the following relationship:

$$\frac{\partial}{\partial x'^{\mu}} = \frac{\partial x^{\nu}}{\partial x'^{\mu}}\frac{\partial}{\partial x^{\nu}} = \hat{\Lambda}^{\nu}_{\mu}\frac{\partial}{\partial x^{\nu}} = \begin{pmatrix} 1 & \beta_j \\ 0 & \delta_{ij} \end{pmatrix}\begin{pmatrix} \dfrac{\partial}{\partial x^0} \\ \dfrac{\partial}{\partial x^j} \end{pmatrix} = \begin{pmatrix} \dfrac{\partial}{\partial x^0} + \boldsymbol{\beta}\cdot\nabla_{\boldsymbol{x}} \\ \dfrac{\partial}{\partial x^i} \end{pmatrix}, \tag{31}$$

i.e.,

$$\begin{cases} \dfrac{\partial}{\partial t'} = \dfrac{\partial}{\partial t} + \boldsymbol{u}\cdot\nabla_{\boldsymbol{x}'}, \\ \nabla_{\boldsymbol{x}'} = \nabla_{\boldsymbol{x}}. \end{cases} \tag{32}$$

Similarly,

$$\frac{\partial}{\partial x^{\mu}} = \frac{\partial x'^{\nu}}{\partial x^{\mu}}\frac{\partial}{\partial x'^{\nu}} = \Lambda^{\nu}_{\mu}\frac{\partial}{\partial x'^{\nu}} = \begin{pmatrix} \dfrac{\partial}{\partial x'^0} - \boldsymbol{\beta}\cdot\nabla_{\boldsymbol{x}'} \\ \dfrac{\partial}{\partial x'^i} \end{pmatrix}, \tag{33}$$

i.e.,

$$\begin{cases} \dfrac{\partial}{\partial t} = \dfrac{\partial}{\partial t'} - \boldsymbol{u}\cdot\nabla_{\boldsymbol{x}'}, \\ \nabla_{\boldsymbol{x}} = \nabla_{\boldsymbol{x}'}. \end{cases} \tag{34}$$

Hence, in various reference frames, while the spatial gradient operator remains constant, the time gradient operator varies. Notably, the substantial derivative in classical fluid theory, derived from the Galilean spacetime transformation, is valid only for low-velocity motion (Song P and Russell, 1999).

In the discussed transformation formulas, the error in the time derivative formula is of the second order of u/c; the error in the space gradient formula is of the first order of u/c.

3.3 Transformations for an Electromagnetic Field in Space Plasmas

This subsection details the transformations of the electromagnetic field in space plasmas among low-speed reference frames.

Space plasmas are typically highly conductive and quasi-neutral. This means that the charge density is extremely low and much less than the current density, i.e., $c\rho \ll j$. For example, in Earth's magnetospheric plasmas, the characteristic values of charge density and current density, as measured by MMS (Burch et al., 2016) and Cluster (Escoubet et al., 2001), are about 10 e/m^3 and 10 nA/m^2, respectively (Tong Y et al., 2018; Argall et al., 2019; Shen C et al., 2021b; Gao L et al., 2024a, b), thus $c\rho/j \sim 10^{-3}$. On the other hand, for slowly varying processes, i.e., when $E/B \ll c$, the electric field is much less than the magnetic field. In Earth's magnetosphere, the characteristic values of the electric field and magnetic field are about 1 mV/m and 100 nT, respectively; thus $E/cB \sim 10^{-3}$. For such low speed situations, with $u \ll c$, the second term in the right-side hand of equation $\boldsymbol{B}' = \boldsymbol{B} - \frac{1}{c^2}\boldsymbol{u}\times\boldsymbol{E}$ in Formula (19) can be neglected. Similarly, the second term in the right-side hand of equation $\boldsymbol{j}' = \boldsymbol{j} - \rho\boldsymbol{u}$ in Formula (23) can be omitted. Therefore, for low speed, high conductive space plasmas, the lower left corner elements in the Lorentz transformation matrix, and its inverse in Equations (15) and (16), are negligible, and the transformation matrix and corresponding inverse matrix are adapted as

$$(\Lambda^{\mu}_{\nu}) = \begin{pmatrix} 1 & -\beta_j \\ 0 & \delta_{ij} \end{pmatrix}, \tag{35}$$

$$(\Lambda^{-1\mu}_{\nu}) = \begin{pmatrix} 1 & \beta_j \\ 0 & \delta_{ij} \end{pmatrix}. \tag{36}$$

Following Equation (4) with the above Lorentz transformation matrix (35), the transformations of electromagnetic potentials between the frames S' and S are described as

$$\begin{pmatrix} \frac{\phi'}{c} \\ A'_i \end{pmatrix} = \begin{pmatrix} 1 & -\beta_j \\ 0 & \delta_{ij} \end{pmatrix} \begin{pmatrix} \frac{\phi}{c} \\ A_j \end{pmatrix} = \begin{pmatrix} \frac{\phi}{c} - \beta_j A_j \\ A_i \end{pmatrix}, \tag{37}$$

i.e.,

$$\begin{cases} \phi' = \phi - \boldsymbol{u}\cdot\boldsymbol{A}, \\ \boldsymbol{A}' = \boldsymbol{A}, \end{cases} \tag{38}$$

or

$$\begin{cases} \phi = \phi' + \boldsymbol{u}\cdot\boldsymbol{A}', \\ \boldsymbol{A} = \boldsymbol{A}'. \end{cases} \tag{39}$$

Thus, in varying reference frames, the observed value of the magnetic vector potential remains unchanged, whereas the value of the electric potential varies. The error in the transformation for electric potential is at the second order of u/c, while the error for the magnetic vector potential is at the first order of u/c.

Under the low speed approximation, and based on the electromagnetic tensor transformation Formula (5) with the Lorentz transformation matrix (35), the transformations for the electric field and magnetic field are derived as follows:

$$\begin{cases} \boldsymbol{E}' = \boldsymbol{E} + \boldsymbol{u}\times\boldsymbol{B}, \\ \boldsymbol{B}' = \boldsymbol{B}, \end{cases} \tag{40}$$

or

$$\begin{cases} \boldsymbol{E} = \boldsymbol{E}' - \boldsymbol{u}\times\boldsymbol{B}', \\ \boldsymbol{B} = \boldsymbol{B}'. \end{cases} \tag{41}$$

This simplification will be accurate to the second order of u/c for the electric field, and the first order of u/c for the magnetic field.

Transformations for electric polarization intensity and magnetic polarization intensity are outlined as well:

$$\begin{cases} \boldsymbol{P}' = \boldsymbol{P} - \frac{1}{c^2}\boldsymbol{u}\times\boldsymbol{M}, \\ \boldsymbol{M}' = \boldsymbol{M}, \end{cases} \tag{42}$$

or

$$\begin{cases} \boldsymbol{P} = \boldsymbol{P}' + \frac{1}{c^2}\boldsymbol{u}\times\boldsymbol{M}', \\ \boldsymbol{M} = \boldsymbol{M}'. \end{cases} \tag{43}$$

Simpified transformations of charge density and electric current density are

$$\begin{pmatrix} \rho' c \\ \boldsymbol{j}' \end{pmatrix} = \begin{pmatrix} 1 & -\boldsymbol{\beta} \\ \boldsymbol{o} & \boldsymbol{I} \end{pmatrix} \cdot \begin{pmatrix} \rho c \\ \boldsymbol{j} \end{pmatrix} = \begin{pmatrix} \rho c - \boldsymbol{\beta}\cdot\boldsymbol{j} \\ \boldsymbol{j} \end{pmatrix}, \tag{44}$$

i.e.,

$$\begin{cases} \rho' = \rho - \boldsymbol{u}\cdot\boldsymbol{j}/c^2, \\ \boldsymbol{j}' = \boldsymbol{j}. \end{cases} \tag{45}$$

Similarly,

$$\begin{pmatrix} \rho c \\ \boldsymbol{j} \end{pmatrix} = \begin{pmatrix} 1 & \boldsymbol{\beta} \\ \boldsymbol{o} & \boldsymbol{I} \end{pmatrix} \cdot \begin{pmatrix} \rho' c \\ \boldsymbol{j}' \end{pmatrix} = \begin{pmatrix} \rho' c + \boldsymbol{\beta}\cdot\boldsymbol{j}' \\ \boldsymbol{j}' \end{pmatrix}, \tag{46}$$

i.e.,

$$\begin{cases} \rho = \rho' + \boldsymbol{u}\cdot\boldsymbol{j}'/c^2, \\ \boldsymbol{j} = \boldsymbol{j}'. \end{cases} \tag{47}$$

In various reference frames, electric current values remain consistent, but charge density may vary. The error in the simplified formulas is limited to the second order of u/c for charge density and the first order of u/c for electric current density.

3.4 Transformations for Wave Frequency and Wave Vector

According to the low speed Lorentz transformation with the transformation matrix (35),

$$\begin{pmatrix} c^{-1}v' \\ \boldsymbol{k}' \end{pmatrix} = \begin{pmatrix} 1 & -\boldsymbol{\beta} \\ \boldsymbol{o} & \boldsymbol{I} \end{pmatrix} \cdot \begin{pmatrix} c^{-1}v \\ \boldsymbol{k} \end{pmatrix} = \begin{pmatrix} c^{-1}v - \boldsymbol{\beta}\cdot\boldsymbol{k} \\ \boldsymbol{k} \end{pmatrix}, \tag{48}$$

we can obtain

$$\begin{cases} v' = v - \boldsymbol{u}\cdot\boldsymbol{k}, \\ \boldsymbol{k}' = \boldsymbol{k}. \end{cases} \tag{49}$$

The discussed formula represents the classical Doppler frequency shift, which assumes negligible variation in the wave vector. This

formula is relevant not only to electromagnetic waves but also to general plasma waves. The Doppler frequency shift is a key tool for measuring the radial velocity of moving objects. In this transformation, the frequency shift error is of the second order of u/c, and the wave vector transformation error is of the first order of u/c.

3.5 Transformations for the Spatial and Temporal Gradients of the Magnetic Field

Based on the transformation relationships derived above, the first-order gradient of a magnetic field can be obtained as follows:

$$\nabla_{\boldsymbol{x}}\boldsymbol{B} = \nabla_{\boldsymbol{x}'}\boldsymbol{B}'. \tag{50}$$

The first-order temporal derivative of a magnetic field is

$$\partial_t\boldsymbol{B} = (\partial_{t'} - \boldsymbol{u}\cdot\nabla_{\boldsymbol{x}'})\boldsymbol{B}' = \partial_{t'}\boldsymbol{B}' - \boldsymbol{u}\cdot\nabla_{\boldsymbol{x}'}\boldsymbol{B}'. \tag{51}$$

When combining (50) and (51), the expression reduces to

$$\partial_t\boldsymbol{B} = \partial_{t'}\boldsymbol{B}' - \boldsymbol{u}\cdot\nabla_{\boldsymbol{x}}\boldsymbol{B}. \tag{52}$$

The second-order gradient of the magnetic field satisfies

$$\nabla_{\boldsymbol{x}}\nabla_{\boldsymbol{x}}\boldsymbol{B} = \nabla_{\boldsymbol{x}'}\nabla_{\boldsymbol{x}'}\boldsymbol{B}', \tag{53}$$

while the temporal derivative of the magnetic field gradient is

$$\partial_t\nabla_{\boldsymbol{x}}\boldsymbol{B} = (\partial_{t'} - \boldsymbol{u}\cdot\nabla_{\boldsymbol{x}'})\nabla_{\boldsymbol{x}'}\boldsymbol{B}' = \nabla_{\boldsymbol{x}'}\partial_{t'}B' - \boldsymbol{u}\cdot\nabla_{\boldsymbol{x}'}\nabla_{\boldsymbol{x}'}\boldsymbol{B}'. \tag{54}$$

Therefore, we can obtain

$$\partial_t\nabla_{\boldsymbol{x}}\boldsymbol{B} = \nabla_{\boldsymbol{x}'}\partial_{t'}B' - \boldsymbol{u}\cdot\nabla_{\boldsymbol{x}}\nabla_{\boldsymbol{x}}\boldsymbol{B}. \tag{55}$$

In the reference frame S', which moves together with the electromagnetic structures, the magnetic field's observed value remains constant over time, i.e., $\dfrac{\partial\boldsymbol{B}'}{\partial t'} = 0$. This establishes a transformation relationship between the satellite observation reference frame S and the electromagnetic structure reference frame S',

$$\begin{cases}\partial_t\boldsymbol{B} = -\boldsymbol{u}\cdot\nabla\boldsymbol{B},\\ \partial_t\nabla\boldsymbol{B} = -\boldsymbol{u}\cdot\nabla\nabla\boldsymbol{B},\end{cases} \tag{56}$$

and

$$\begin{cases}\nabla\boldsymbol{B} = \nabla'\boldsymbol{B}',\\ \nabla\nabla\boldsymbol{B} = \nabla'\nabla'\boldsymbol{B}'.\end{cases} \tag{57}$$

Therefore, the gradient of magnetic field is the same in different reference frames. Utilizing multi-point magnetic measurements from multi-satellite constellations such as Cluster (Escoubet et al., 2001) or MMS (Burch et al., 2016), one can derive the magnetic field's temporal variation rate and first-order spatial gradient (Harvey, 1998; Chanteur, 1998). Subsequently, Equation (56) facilitates calculation of velocities of electromagnetic structures relative to the constellations (Shi QQ et al., 2006; Shen C et al., 2021a), along with the nine components of the second-order magnetic gradient (Shen C et al., 2021a). Additionally, Equation (56) can determine the three components of the first-order magnetic gradient along the motion direction, assuming that the electromagnetic structure's velocity is already known (Shen C et al., 2012). It is important to note that Equations (56) and (57) apply both to inertial and to non-inertial reference frames, thus remaining valid even for electromagnetic structures undergoing unsteady, accelerated, or expansive motion.

For low-speed physical processes in space plasmas, the Coulomb gauge constrains the magnetic vector potential in reference frame S

$$\nabla\cdot\boldsymbol{A} = 0. \tag{58}$$

In another arbitrary reference frame S', combining Equations (32) and (38) reduces to

$$\nabla'\cdot\boldsymbol{A}' = 0. \tag{59}$$

This yields a result consistent with the Coulomb gauge. This indicates that the Coulomb gauge remains valid in any low-speed reference frame, suggesting that an electromagnetic structure's charge density and electric scalar potential will follow the Poisson equation.

It is crucial to recognize that the transformations of spacetime, spacetime gradient, and electromagnetic field are valid locally between both non-inertial and inertial reference frames. These transformation formulas are highly practical whenever first-order errors of u/c are negligible. It can be shown that the equations of magnetohydrodynamics applicable for low velocity motions are compatible with Galilean transformations in non-inertial frames of references.

However, for high-speed motions, the previously discussed approximations are not suitable. For instance, the phase velocity of plasma waves can often reach or exceed the speed of light. Consequently, this velocity cannot be accurately determined using the methods previously mentioned (Shi QQ et al., 2006). In the case of high-energy particles within the radiation belts, their bounce motion along a geomagnetic field line can approach the speed of light (Ni B et al., 2018; Li YX et al., 2023). In such scenarios, the relative velocities of reference systems are also near the speed of light, necessitating the use of Equations (9)–(12) from Section 2 for the transformation of electromagnetic fields from one reference frame to another.

It is worth noting that the low speed transformation relations derived above provide a natural theoretical foundation for applying the seven-spacecraft (seven-point) analysis method proposed for the plasma observation mission (Shen C et al., 2025). In particular, the invariance of the magnetic field gradient under reference frame transformations, and the coupling between temporal derivatives and spatial gradients, enable inference—directly from time series measurements—of the apparent velocity of electromagnetic structures and the longitudinal components of the quadratic magnetic gradient. When combined with the non-planar dual-tetrahedral configuration of the seven spacecraft, these transformation constraints supply the additional degrees of freedom required to reconstruct both first and second order spatial gradients of the magnetic field using a least squares approach. As a result, the framework developed here is well suited for studying three dimensional, nonlinear plasma structures with the planned seven point constellation, extending traditional multi-spacecraft gradient techniques beyond the linear approximation.

4. Corotational Potential of Planets with Intrinsic Magnetic Fields

This section demonstrates the practical application of Galilean transformations to the electromagnetic field as discussed.

Several planets, including Earth, Jupiter, Saturn, Uranus, and Neptune, possess intrinsic magnetic fields that are primarily dipolar. These dipole magnetic fields rotate with the planet, inducing a corotation electric field. This electric field plays a crucial role in the dynamics of the planet's plasmasphere (Lemaire et al., 1998; Ti S et al., 2021) and the evolution of ring current energetic particles during magnetic storms (Fok et al., 2001; Shen C and Liu ZX, 2002). Understanding the spatial distribution of a planet's corotation electric field and its potential is vital for studying the dynamics of the planet's plasmasphere and ring current during geomagnetic storms. Parks (1991) developed a method to calculate the corotation potential, assuming that a planet's magnetic core and its centroid coincide. However, it has been observed that the magnetic cores of planets often deviate from their centroids. Here, we present a general expression for the corotation potential of planets with intrinsic magnetic fields and rotation.

In a reference system centered at the magnetic core, the dipole magnetic field of a planet is given by

$$\boldsymbol{B}' = \frac{3\boldsymbol{r}'(\boldsymbol{r}'\cdot\boldsymbol{M}) - r'^2\boldsymbol{M}}{r'^5}, \tag{60}$$

where $\boldsymbol{M}$ is the dipole moment, and $\boldsymbol{r}'$ is the position vector starting from the magnetic core O. The corresponding magnetic vector potential is described as follows:

$$\boldsymbol{A}' = \frac{\boldsymbol{M}\times\boldsymbol{r}'}{r'^3}. \tag{61}$$

Two reference frames are considered: (1) the corotating reference frame of the planet, in which the intrinsic magnetic field is stationary, and (2) the planetary centroid reference frame, which is nonrotating and in which the planet rotates with angular velocity $\boldsymbol{\Omega}$. Let C denote the planetary centroid, which is connected with the magnetic core O by the vector $\boldsymbol{R}_0$. Therefore, for an arbitrary observation point, its position vector $\boldsymbol{R}$ relative to C equates $\boldsymbol{R}_0+\boldsymbol{r}'$, as illustrated in Figure 1. Given the slow rotation of our solar system's planets, the relative velocities ($\boldsymbol{u}=\boldsymbol{\Omega}\times\boldsymbol{R}$) are significantly less than the speed of light, allowing the use of Galilean transformations as described above. (Under Galilean transformation, the position vectors remain unchanged in different reference frames.) In the reference frame of the planet's centroid, it follows from Equations (39) and (40) that $\boldsymbol{A}=\boldsymbol{A}'$ and $\boldsymbol{B}=\boldsymbol{B}'$, i.e., the magnetic field strength and magnetic vector potential, remain consistent with those in the corotation reference frame. According to Equation (41), the corotation electric field observed in the planetary centroid reference frame is

$$\boldsymbol{E}_{\rm cor} = -\boldsymbol{u}\times\boldsymbol{B}' = -(\boldsymbol{\Omega}\times\boldsymbol{R})\times\boldsymbol{B}'. \tag{62}$$

According to Equation (39), the corotation potential observed in the planetary centroid reference frame is defined as

$$\begin{aligned}\phi_{\rm cor} &= \boldsymbol{u}\cdot\boldsymbol{A}' = (\boldsymbol{\Omega}\times\boldsymbol{R})\cdot\boldsymbol{A}' = \frac{1}{r'^3}(\boldsymbol{\Omega}\times\boldsymbol{R})\cdot(\boldsymbol{M}\times\boldsymbol{r}')\\ &= \frac{1}{r'^3}\left[(\boldsymbol{M}\cdot\boldsymbol{\Omega})(\boldsymbol{R}\cdot\boldsymbol{r}') - (\boldsymbol{M}\cdot\boldsymbol{R})(\boldsymbol{\Omega}\cdot\boldsymbol{r}')\right].\end{aligned} \tag{63}$$

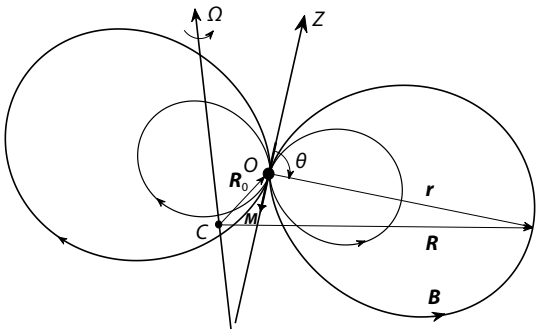

Figure 1. Schematic diagram of a planet's dipole magnetic field rotating along with the planet. The centroid of the planet is marked as C, and the planet has rotation angular velocity $\boldsymbol{\Omega}$; $\boldsymbol{R}$ is the vector from the centroid of planet C. The planet has a dipole moment $\boldsymbol{M}$ with its magnetic core located at point O. $\boldsymbol{R}_0$ is the vector from centroid C to magnetic core O.

If the magnetic core coincides with the planetary centroid ($\boldsymbol{R}_0=0$) and the magnetic moment is aligned with the rotation axis ($\boldsymbol{\Omega}//\boldsymbol{M}$), then the expression simplifies to

$$\phi_{\rm cor} = \frac{\Omega M\sin^2\theta'}{r'} = \frac{\Omega M}{La}, \tag{64}$$

where a is the radius of the planet and L denotes the magnetic shell index (a parameter that labels a geomagnetic field line by its equatorial distance from Earth's center, measured in Earth radii). Equation (64) demonstrates that the magnetic field lines are equipotential lines. Furthermore, on the drift surface with a consistent magnetic shell index L, the corotation potential remains constant.

It follows from Equation (47) that if the charge density and current density are zero in the corotation reference frame, they will also be zero when measured in the geocentric stationary reference frame. However, the derived corotation electric field and potential exhibit a first-order error in u/c. Consequently, the divergence of the corotation electric field, as described by Equation (62), is not strictly zero because

$$\nabla\cdot\boldsymbol{E}_{\rm cor} = \nabla\cdot(\boldsymbol{u}\times\boldsymbol{B}') = \boldsymbol{B}'\cdot(\nabla\times\boldsymbol{u}) - \boldsymbol{u}\cdot(\nabla\times\boldsymbol{B}') = \boldsymbol{B}'\cdot\boldsymbol{\omega}, \tag{65}$$

where $\nabla\times\boldsymbol{B}' = \nabla'\times\boldsymbol{B}' = \mu_0\boldsymbol{j}' = 0$ is used and zero current density is assumed except in the magnetic core. Considering the vorticity $\boldsymbol{\omega} = \nabla\times\boldsymbol{u} = \nabla\times(\boldsymbol{\Omega}\times\boldsymbol{R}) = 2\boldsymbol{\Omega}$, Equation (65) becomes

$$\nabla\cdot\boldsymbol{E}_{\rm cor} = 2\boldsymbol{B}'\cdot\boldsymbol{\Omega}. \tag{66}$$

For Earth, the charge density error approaches the measurement threshold of MMS (Shen C et al., 2021b), indicating that Gauss's law might not be strictly applicable. This discrepancy arises because the corotation electric field, under the Galilean transformation, carries a first-order error proportional to $u/c\sim\Omega R/c$. Therefore, calculations involving charge density should consider use of more accurate transformations than the Galilean transformations, such as the Lorentz transformation detailed in Equations (18) to (24).

The planetary magnetic field comprises not only the dipole magnetic field, but also higher magnetic pole moment compo-

nents, such as the magnetic dipole moment $\boldsymbol{M}_1$, quadrupole moment $\boldsymbol{M}_2$, octupole moment $\boldsymbol{M}_3$, etc. When the magnetic vector potentials for each class of magnetic moments ($\boldsymbol{A}_1$,$\boldsymbol{A}_2$,…) are provided, the planet's total magnetic vector potential can be determined,

$$\boldsymbol{A} = \boldsymbol{A}_1 + \boldsymbol{A}_2 + \boldsymbol{A}_3 + \cdots. \tag{67}$$

Higher order magnetic moments decay more rapidly with distance than does the dipole term and are therefore important primarily in near-planet regions with strong magnetic gradients. For Earth, the dipole component dominates beyond a few planetary radii, while quadrupole and higher order terms may introduce localized corrections in the inner magnetosphere. The Formulation (67) naturally accommodates these higher order contributions through linear superposition of the magnetic vector potential.

In interplanetary space, where external fields are not considered, the magnetic field satisfies a specific condition $\nabla \times \boldsymbol{B} = 0$, leading to a conclusion about magnetic scalar potential $\boldsymbol{B} = -\nabla U$. Due to $\nabla \cdot \boldsymbol{B} = 0$, the magnetic scalar potential satisfies $\nabla^2 U = 0$. This allows for the internal magnetic field of planets to be represented through a series of spherical harmonics (Jordan, 1994):

$$U = a\sum_{n=1}^{\infty}\sum_{m=0}^{n}\left(\frac{a}{r}\right)^{n+1}\left[g_n^m\cos(m\varphi) + h_n^m\sin(m\varphi)\right]P_n^m(\cos\theta), \tag{68}$$

where a is the planetary radius, θ is the geographical latitude, φ is the geographic longitude, $P_n^m(\cos\theta)$ is the associated Legendre polynomial with n-order and m-degree, and g_n^m and h_n^m are Gauss coefficients.

For the case $n = 1$, the magnetic scalar potential is

$$U_1 = \frac{a^3}{r^2}\left[g_1^0\cos\theta + \left(g_1^1\cos\varphi + h_1^1\sin\varphi\right)\sin\theta\right]. \tag{69}$$

The magnetic scalar potential for the dipole moment is

$$U_1 = -\frac{M\cos\theta'}{r^2}. \tag{70}$$

The planetary dipole moment $M_1 = a^3\sqrt{\left(g_1^0\right)^2 + \left(g_1^1\right)^2 + \left(h_1^1\right)^2}$, along with the quadrupole and octupole moments provided by Antipov and Tikhonov (2013), are crucial for understanding Earth's magnetic field, though the significance of higher-order moments remains to be resolved.

Additionally, the concept of corotation potential is introduced in the context of the planetary centroid reference frame.

$$\phi_{cor} = \boldsymbol{u}\cdot\boldsymbol{A} = (\boldsymbol{\Omega}\times\boldsymbol{R})\cdot(\boldsymbol{A}_1 + \boldsymbol{A}_2 + \boldsymbol{A}_3 + \cdots). \tag{71}$$

5. Charge Density Measurements by Spacecraft Constellations

Multiple-spacecraft constellations are crucial for exploring the three-dimensional characteristics of electromagnetic structures in space, such as flux ropes, the magnetopause boundary layer, and current sheets (Escoubet et al., 2001; Burch et al., 2016; Torbert et al., 2016). These constellations can measure the spatial gradient of the electrostatic field (Chanteur, 1998), allowing for use of the Gaussian law to determine the charge density in static electromagnetic structures (Tong Y et al., 2018; Argall et al., 2019; Shen C et al., 2021b). However, these electromagnetic structures are often dynamic, and move relative to the spacecraft constellation. It remains an unsolved problem whether the charge density in moving electromagnetic structures, with their time-varying fields, can be determined accurately from electrostatic field measurements made from spacecraft in a constellation. Additionally, relative motions between the satellites can affect electric field measurements and potentially lead to inaccuracies in charge density calculations.

Building on theoretical findings discussed in the previous section, this section rigorously evaluates the feasibility of, and potential errors in, calculations of charge density based on such electrostatic field measurements made by spacecraft constellations. Our analysis involves transformations among four different reference frames: the spacecraft rotational reference frames, the spacecraft centroid reference frames, the constellation centroid reference frame, and the reference frame moving with the electromagnetic structure. The spacecraft rotational frames are non-inertial. The spacecraft centroid frames, being in free fall within Earth's gravity, can be considered as local inertial frames. The constellation centroid frame may be rotational due to relative spacecraft motions, and the frame moving with the electromagnetic structure may also be non-inertial if the structure is accelerating or decelerating. Due to the relatively low speeds of macro motions in space, the Galilean transformations discussed in Section 4 are deemed sufficiently accurate.

In space explorations, electric field measurements typically utilize the two-probe method, as depicted in Figure 2. This method involves recording the potential difference between two probes to determine the electric field component aligned with the probes. By evaluating the potentials detected at three non-parallel probe pairs, the vector components of the electric field can be

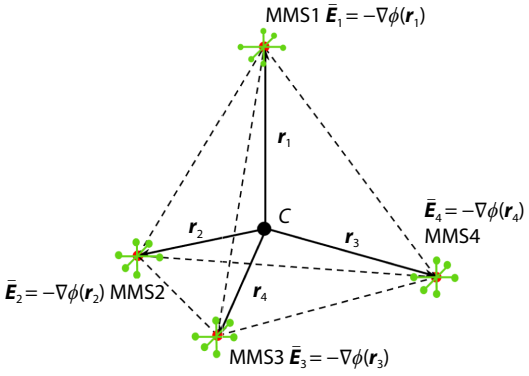

Figure 2. Schematic diagram of the space electric field measurements by MMS (Magnetospheric Multiscale; Burch et al., 2016). The centroid of the four spacecrafts of MMS is at point C. Thus, in the constellation centroid reference frame with C as its origin, the position vectors of the four satellites are $\boldsymbol{r}_\alpha$ (α = 1, 2, 3, 4), while $\boldsymbol{r}_c = \frac{1}{4}\sum_{\alpha=1}^{4}\boldsymbol{r}_\alpha = 0$. Provided by the 6-probe potential measurements of each spacecraft, the electrostatic fields $\bar{\boldsymbol{E}}_s(\boldsymbol{r}_\alpha) = -\nabla_s\tilde{\phi}(\boldsymbol{r}_\alpha)$, ($\alpha$ = 1, 2, 3, 4) at the 4 satellites are readily yielded (Harvey, 1998; Shen C et al., 2003).

ascertained. However, to measure the weak electric field (~mV/m) in space, it is common practice to extend the distance between the potential-probes by exploiting the centrifugal force generated by the satellite's rotation. These measurements are taken within the spacecraft's rotational reference frame $\tilde{K}$, where time and space coordinates are denoted as $(\tilde{t}, \tilde{\boldsymbol{r}})$, electric potential field as $\tilde{\phi}(\tilde{t}, \tilde{\boldsymbol{r}})$, magnetic vector potential by $\tilde{\boldsymbol{A}}(\tilde{t}, \tilde{\boldsymbol{r}})$, and other physical quantities are indicated by "~". The electric field observed in this frame $\tilde{K}$ is thus defined,

$$\tilde{\boldsymbol{E}} = -\nabla_{\tilde{\boldsymbol{r}}}\tilde{\phi} - \frac{\partial}{\partial \tilde{t}}\tilde{\boldsymbol{A}}. \tag{72}$$

The electric field at the spacecraft centroid O measured in the frame $\tilde{K}$ is

$$\tilde{\boldsymbol{E}}_o = -(\nabla_{\tilde{\boldsymbol{r}}}\tilde{\phi})_o - \frac{\partial}{\partial \tilde{t}}\tilde{\boldsymbol{A}}_o. \tag{73}$$

The spacecraft's centroid reference frames K_s are non-rotational and move along with the spacecraft's centroids, where time and space coordinates are represented as $(t_s, \boldsymbol{r}_s)$, and a subscript 's' is added to each physical quantity to denote this frame. The relative velocity between the satellite rotation reference frame $\tilde{K}$ and the spacecraft centroid reference frames K_s at the spacecraft centroids is $\boldsymbol{w} = \boldsymbol{\Omega} \times (\boldsymbol{r}_s - \boldsymbol{r}_0) = 0$. Therefore, all physical quantities measured at the satellite's centroid in these two different reference frames are identical and $\frac{\partial}{\partial t_s} = \frac{\partial}{\partial \tilde{t}}$, as previously explained. In the spacecraft centroid reference frames K_s, the electric field at the centroid is denoted as $\boldsymbol{E}_s = \tilde{\boldsymbol{E}}_0 = -(\nabla_{\tilde{\boldsymbol{r}}}\tilde{\phi})_0 - \frac{\partial}{\partial \tilde{t}}\tilde{\boldsymbol{A}}_0$,

$$\boldsymbol{E}_s = -(\nabla_s\tilde{\phi}) - \frac{\partial}{\partial t_s}\boldsymbol{A}_s = \overline{\boldsymbol{E}}_s - \frac{\partial}{\partial t_s}\boldsymbol{A}_s, \tag{74}$$

where the electrostatic field is labeled as $\overline{\boldsymbol{E}}_s \equiv -\nabla_s\tilde{\phi}$. It is important to note that, currently, only this DC electrostatic field can be detected through practical space measurements.

In addition to bulk movements of a spacecraft constellation, its measurements can be influenced also by any relative motions among its members. In the constellation centroid reference frame K, time and space coordinates are expressed as $(t, \boldsymbol{r})$, and the velocity of each spacecraft relative to the centroid C is $\boldsymbol{v}$. The electric field observed at each spacecraft centroid in frame K is denoted as

$$\boldsymbol{E} = \boldsymbol{E}_s - \boldsymbol{v} \times \boldsymbol{B} = \overline{\boldsymbol{E}}_s - \frac{\partial}{\partial t_s}\boldsymbol{A}_s - \boldsymbol{v} \times \boldsymbol{B} = \overline{\boldsymbol{E}} - \frac{\partial}{\partial t_s}\boldsymbol{A}_s, \tag{75}$$

where the electrostatic field observed in the constellation centroid frame K is

$$\overline{\boldsymbol{E}} \equiv \overline{\boldsymbol{E}}_s - \boldsymbol{v} \times \boldsymbol{B}. \tag{76}$$

Then the charge density measured in K can be calculated from Gauss's law as

$$\varepsilon_0^{-1}\rho = \nabla \cdot \boldsymbol{E} = \nabla \cdot \overline{\boldsymbol{E}} - \nabla \cdot \left(\frac{\partial}{\partial t_s}\boldsymbol{A}_s\right), \tag{77}$$

where

$$\nabla \cdot \left(\frac{\partial}{\partial t_s}\boldsymbol{A}_s\right) = \nabla_s \cdot \left(\frac{\partial}{\partial t_s}\boldsymbol{A}_s\right) = \frac{\partial}{\partial t_s}\nabla_s \cdot \boldsymbol{A}_s. \tag{78}$$

Here, the relationship $\nabla = \nabla_s$ has been applied. As derived in Section 3.5, the Coulomb gauge is effective in every reference frame for low-speed electromagnetic structures in space, leading to $\nabla \cdot \boldsymbol{A} = \nabla_s \cdot \boldsymbol{A}_s = 0$. Consequently, Equation (78) simplifies to $\nabla \cdot \left(\frac{\partial}{\partial t_s}\boldsymbol{A}_s\right) = 0$, and the second term on the right side of Equation (77) becomes null. Therefore, calculation of the charge density observed in the constellation centroid frame K can be described as

$$\rho = \varepsilon_0\left(\nabla \cdot \overline{\boldsymbol{E}}\right)_c. \tag{79}$$

This indicates that the charge density at the constellation's centroid can be calculated directly from the electrostatic field measurements at each spacecraft in low-speed situations, without requiring measurement of the magnetic vector potential; use of Galilean transformations introduces only a negligible first-order error of u/c to Formula (79).

Previous studies have overlooked the impact on electric field measurements of the relative motions of spacecraft (Tong Y et al., 2018; Argall et al., 2019; Shen C et al., 2021b). Equation (76) reveals that correction for the electrostatic field $-\boldsymbol{v} \times \boldsymbol{B}$ is appropriate, and thus we add it to Equation (79) to correct the calculation of charge density to account for the relative motion of the spacecraft:

$$\varepsilon_0\nabla \cdot (-\boldsymbol{v} \times \boldsymbol{B}) = -\varepsilon_0\boldsymbol{B} \cdot (\nabla \times \boldsymbol{v}) + \varepsilon_0\boldsymbol{v} \cdot \nabla \times \boldsymbol{B} = \varepsilon_0\boldsymbol{B} \cdot \boldsymbol{\omega}. \tag{80}$$

Here, the vorticity of the constellation is $\boldsymbol{\omega} = \nabla \times \boldsymbol{v}$; at the constellation's centroid $\boldsymbol{v} = 0$, the vorticity of the constellation $\boldsymbol{\omega}$ is usually small, suggesting that the relative motion of satellites within the constellation negligibly affects the charge density. However, as the constellation approaches Earth, both the magnetic field and the vorticity increase, leading to a greater deviation in charge density $\varepsilon_0\boldsymbol{B} \cdot \boldsymbol{\omega}$. As reported in our previous study of inner magnetospheric charge distribution (Gao L et al., 2024a), the uncorrected charge density exhibits an anomalous increase as MMS approaches Earth and the magnetic field strength grows substantially. Therefore, these data require correction by $\varepsilon_0\boldsymbol{B} \cdot \boldsymbol{\omega}$.

An electromagnetic structure moving relative to the constellation at speed $\boldsymbol{v}$ has its proper reference frame denoted as 'K''. The relative velocities of electromagnetic structures in space are typically much smaller than the speed of light in a vacuum, making Galilean transformations approximately valid. By applying transformation relationship (45), the intrinsic charge density in the proper reference frame moving with the electromagnetic structure can be determined from the charge density and current density measured in the reference frame of the constellation's centroid:

$$\rho' = \rho - \frac{1}{c^2}\boldsymbol{V} \cdot \boldsymbol{j} = \varepsilon_0\left(\nabla \cdot \overline{\boldsymbol{E}}\right)_c - \frac{1}{c^2}\boldsymbol{V} \cdot \boldsymbol{j}. \tag{81}$$

The current density of the electromagnetic structure in the constellation reference system can be measured by particle detectors ($\boldsymbol{j} = \sum_i q_i n_i \boldsymbol{v}_i$) (Paschmann et al., 1998) or derived from Ampere's Law using multi-point magnetic field measurements of the constellations (Dunlop et al., 1988). The second term on the right-hand side of the formula is usually insignificant and can be disregarded, which means there were no significant issues in previous calculations of charge density (Tong Y et al., 2018; Argall et al.,

2019; Shen C et al., 2021b; Gao L et al., 2024a).

As demonstrated, the method of calculating the charge density at the constellation's centroid using electrostatic field measurements from each spacecraft is rigorously validated, with the error being at the first order of u/c.

6. Conclusions

When addressing space physics challenges, it often becomes necessary to convert electromagnetic field quantities across different reference frames. This topic has been explored in various dissertations by researchers in the field of space physics (Parks, 1991; Song P and Russell, 1999). This paper, however, focuses on a systematic investigation of the transformation of electromagnetic fields between different reference frames in space, presenting basic results that have broad applicability.

In space's non-inertial reference frames, the equivalent gravity is relatively weak, causing only minor distortions in spacetime ($\sim 10^{-13}$). This allows the physical laws of flat spacetime to remain accurate with high precision. The Lorentz transformation is suitable for electromagnetic field transformations between any reference frames, whether inertial or non-inertial. For non-inertial frames, it is critical that the simplified equations presented here by used only when the relative velocity between frames is significantly lower than the speed of light, thus limiting truncation errors to the second order of u/c. For typical motions that satisfy this definition of "low speed", Formulas (13)–(21), which use first-order approximations, are recommended.

The concept of absolute space and time proves useful in studying macroscopic dynamics in space, particularly under conditions of low-speed motion where the relative speed is much less than the speed of light. In this absolute framework, the length of a ruler and the clock timing remain constant across different reference frames. This paper has provided a detailed discussion of Galilean transformations of electromagnetic field quantities between reference frames and has examined their application limits. We have presented illustrative examples in which we apply the approximate transformations. Equations (56) and (57) introduce a concise relationship between the temporal variation rate of the magnetic field, the magnetic gradient, and the apparent velocity of the electromagnetic structure speeds low compared to the speed of light. These equations are useful for estimating the apparent velocity of electromagnetic structures (Shi QQ et al., 2006; Shen C et al., 2021a) and the components of first or second order magnetic gradients (Shen C et al., 2012, 2021a) in analyses of data from multiple spacecraft.

This study has also derived a general formula for the planetary corotation electric field using the Galilean transformation formulas for electromagnetic fields, applicable under general conditions where the magnetic core is offset from the axis of planetary rotation.

Lastly, this investigation confirms the feasibility of calculating the charge density of electromagnetic structures using electrostatic field measurements from spacecraft constellations. We have shown that the Poisson equation remains valid under first-order u/c approximations, which means that electrostatic field observations by the MMS constellation can be used to deduce charge density in any low-speed moving electromagnetic structures with reasonable accuracy.

Acknowledgments

This work was supported by the National Natural Science Foundation of China (Grants No. 42130202 (CS), 42564008 (YJ)), and the National Key Research and Development Program of China (Grant No. 2022YFA1604600 (CS)). This research was also supported by the Shenzhen Technology Project (Grant no. JCYJ20241202123905008), Ningxia Natural Science Foundation (No. 2024AAC03080) and the International Space Science Institute (ISSI) in Bern, through ISSI International Team project #556 (Cross-scale energy transfer in space plasmas). Thanks to Peng Shao and Lai Gao for the help on the plots. The authors appreciate the valuable suggestions made by reviewers.

Author contributions

Chao Shen: Conceptualization; Investigation and analysis; Methodology; Writing–original draft, review & editing (equal); Figure drawing; Funding acquisition; Supervision.
Yong Ji: Writing–review & evaluation (equal).

Competing interests

The contact author has declared that neither of the authors has any competing interests.

Data availability

This paper mainly carries out a theoretical investigation. The data sets analyzed during the current density and charge density estimations were obtained from the MMS Science Data Center (https://lasp.colorado.edu/mms/sdc/public/), including magnetic fields from the Fluxgate Magnetometers (FGM) and the Electric field Double Probe (EDP). The authors thank the MMS field teams for providing these high-quality data.

References

Antipov, K. A., and Tikhonov, A. A. (2013). Multipole models of the geomagnetic field: Construction of the Nth approximation. *Geomagn. Aeron*. 53, 257–267. https://doi.org/10.1134/S0016793213020023

Argall, M. R., Shuster, J. R., Dors, I., Genestreti, K. J., Nakamura, T. K. M., Torbert, R. B., Webster, J. M., Ahmadi, N., Ergun, R., Strangeway, R. J., Giles, B. L., and Burch, J. (2019). How neutral is quasi-neutral: Charge density in the reconnection diffusion region observed by MMS. AGU Fall Meeting 2019, San Francisco, CA, United States. Abstract SM21B-3153.

Burch, J. L., Moore, T. E., Torbert, R. B., and Giles, B. L. (2016). Magnetospheric multiscale overview and science objectives. *Space Sci. Rev.*, *199*(1–4), 5–21. https://doi.org/10.1007/s11214-015-0164-9

Chanteur, G., and Harvey, C. C. (1998). Spatial interpolation for four spacecraft: Application to magnetic gradients. In ISSI Scientific Reports Series(Vol. 1, pp. 371–394).

D'Auria, R., and Trigiante, M. (2011). *From Special Relativity to Feynman Diagrams* (p. 144). Berlin: Springer.

Dunlop, M. W., Southwood, D. J., Glassmeier, K. H., and Neubauer, F. M. (1988). Analysis of multipoint magnetometer data. *Adv. Space Res.*, *8*(9–10), 273–277. https://doi.org/10.1016/0273-1177(88)90141-x

Escoubet, C. P., Fehringer, M., and Goldstein, M. (2001). *Introduction* the cluster

mission. *Ann. Geophys.*, *19*(10-12), 1197–1200. https://doi.org/10.5194/angeo-19-1197-2001

Fok, M. C., Wolf, R. A., Spiro, R. W., and Moore, T. E. (2001). Comprehensive computational model of Earth's ring current. *J. Geophys. Res.: Space Phys.*, *106*(A5), 8417–8424. https://doi.org/10.1029/2000JA000235

Gao, L., Shen, C., Zhou, Y. F., Ji, Y., Pu, Z. Y., Parks, G., Russell, C. T., Zeng, G., Ma, L., … Burch, J. L. (2024a). Observational features of charge distribution in Earth's inner magnetosphere. *Commun. Phys.*, *7*(1), 63. https://doi.org/10.1038/s42005-024-01553-5

Gao, L., Shen, C., Ji, Y., Zhou, Y. F., and Bogdanova, Y. V. (2024b). The electric properties of the magnetopause boundary layer. *Magnetochemistry*, *10*(6), 37. https://doi.org/10.3390/magnetochemistry10060037

Harvey, C. C. (1998). Spatial gradients and the volumetric tensor. In G. Paschmann and P. W. Daly (Eds.), *Analysis methods for multi-spacecraft data* (pp. 307–322). ISSI Scientific Reports Series. (ISSI Scientific Report No. SR-001).

Jordan, C. E. (1994). Empirical models of the magnetospheric magnetic field. *Rev. Geophys.*, *32*(2), 139–157. https://doi.org/10.1029/94RG00100

Lemaire, J. F., Gringauz, K. I., Carpenter, D. L., and Bassolo, V. (1998). *The Earth's Plasmasphere* (pp. 272–273). Cambridge: Cambridge University Press. https://doi.org/10.1017/CBO9780511600098

Li, Y. X., Yue, C., Liu, Y., Zong, Q.-G., Zou, H., and Ye, Y. G. (2023). Dynamics of the inner electron radiation belt: A review. *Earth and Planetary Physics*, *7*(1), 109–118. https://doi.org/10.26464/epp2023009

Misner, C.W., Thorne, K.S., and Wheeler, J.A. (1973). *Gravitation*, San Francisco: W.H. Freeman.

Ni, B., Huang, J., Ge, Y., Cui, J., Wei, Y., Gu, X., Fu, S., Xiang, Z., and Zhao, Z. (2018). Radiation belt electron scattering by whistler-mode chorus in the Jovian magnetosphere: Importance of ambient and wave parameters. *Earth and Planetary Physics*, *2*(1), 1–14. https://doi.org/10.26464/epp2018001

Padmanabhan, T. (2010). *Gravitation: Foundations and Frontiers* (p. 272). Cambridge: Cambridge University Press. https://doi.org/10.1017/CBO9780511807787

Parks, G. K. (1991). *Physics of Space Plasmas: an Introduction* (pp. 39–46). Redwood City: Addison-Wesley.

Paschmann, G., Fazakerley, A. N., and Schwartz, S. J. (1998). Moments of plasma velocity distributions. In G. Paschmann, et al. (Eds.), *Analysis Methods for Multi-spacecraft Data* (pp. 125–127). Noordwijk: European Space Agency Publications Division.

Shen, C., and Liu, Z. X. (2002). Properties of the neutral energetic atoms emitted from Earth's ring current region. *Phys. Plasmas*, *9*(9), 3984–3994. https://doi.org/10.1063/1.1500736

Shen, C., Li, X., Dunlop, M., Liu, Z. X., Balogh, A., Baker, D. N., Hapgood, M., and Wang, X. (2003). Analyses on the geometrical structure of magnetic field in the current sheet based on cluster measurements. *J. Geophys. Res. Space Phys.*, *108*(A5), 1168. https://doi.org/10.1029/2002JA009612

Shen, C., Rong, Z. J., and Dunlop, M. (2012). Determining the full magnetic field gradient from two spacecraft measurements under special constraints. *J. Geophys. Res.: Space Phys.*, *117*(A10), A10217. https://doi.org/10.1029/2012JA018063

Shen, C., Zhang, C., Rong, Z. J., Pu, Z. Y., Dunlop, M. W., Escoubet, C. P., Russell, C. T., Zeng, G., Ren, N., … Zhou, Y. F. (2021a). Nonlinear magnetic gradients and complete magnetic geometry from multispacecraft measurements. *J. Geophys. Res.: Space Phys.*, *126*(8), e2020JA028846. https://doi.org/10.1029/2020JA028846

Shen, C., Zhou, Y. F., Gao, L., Wang, X. G., Pu, Z. Y., Escoubet, C. P., and Burch, J. L. (2021b). Measurements of the net charge density of space plasmas. *J. Geophys. Res.: Space Phys.*, *126*(12), e2021JA029511. https://doi.org/10.1029/2021JA029511

Shen, C., Zeng, G., Kieokaew, R., and Zhou, Y. F. (2025). Quadratic magnetic gradients from seven- and nine-spacecraft constellations. *Ann. Geophys.*, *43*(1), 115–135. https://doi.org/10.5194/angeo-43-115-2025

Shi, Q. Q., Shen, C., Dunlop, M. W., Pu, Z. Y., Zong, Q. G., Liu, Z. X., Lucek, E., and Balogh, A. (2006). Motion of observed structures calculated from multi-point magnetic field measurements: Application to cluster. *Geophys. Res. Lett.*, *33*(8), L08109. https://doi.org/10.1029/2005GL025073

Song, P., and Russell, C. T. (1999). Time series data analyses in space physics. *Space Sci. Rev.*, *87*(3), 387–463. https://doi.org/10.1023/A:1005035800454

Ti, S., Shen, C., Chen, T., Ji, Y., He, H., Xu, R. L., and Huang, Y. (2021). Influence of continuous magnetic activities on the evolution of the plasmasphere. *Chin. J. Space Sci. (in Chinese)*, *41*(6), 869–880. https://doi.org/10.11728/cjss2021.06.869

Tong, Y., Vasko, I., Mozer, F. S., Bale, S. D., Roth, I., Artemyev, A. V., Ergun, R., Giles, B., Lindqvist, P. A., … Torbert, R. B. (2018). Simultaneous multispacecraft probing of electron phase space holes. *Geophys. Res. Lett.*, *45*(21), 11513–11519. https://doi.org/10.1029/2018GL079044

Torbert, R. B., Russell, C. T., Magnes, W., Ergun, R. E., Lindqvist, P. A., Lecontel, O., Vaith, H., Macri, J., Myers, S., … Lappalainen, K. (2016). The FIELDS instrument suite on MMS: Scientific objectives, measurements, and data products. *Space Sci. Rev.*, *199*(1), 105–135. https://doi.org/10.1007/s11214-014-0109-8